Proc Indian Natn Sci Acad, **70, A,** No. 3, May 2004, pp. 489-502

PERFORMANCE EVALUATION OF A STANDARD MOLTEN CARBONATE FUEL CELL AT DIFFERENT OPERATING CONDITIONS

G PRABHU, C SOLAIYAN, S DHEENADAYALAN, R CHANDRASEKARAN AND R PATTABIRAMAN*

Central Electrochemical Research Institute, Karaikudi-630 006 (India)

(Received 12 December 2002 ; Accepted 24 March 2003)

Single cells of Molten Carbonate fuel cells (MCFC) with an effective area of 3 cm^2 were operated. Pre-sintered Ni-10 wt% Cr anode, *in situ* lithiated nickel oxide cathode and an unsintered tape of lithium aluminate matrix were employed. The electrolyte employed was a eutectic mixture of Li_2CO_3 + K_2CO_3 (62:38 mol%). The cell was operated for 500 hours using standard gas compositions of H_2 + CO_2 (80:20) as fuel and O_2 + CO_2 (67:33) as oxidant. The performance of the cells at various temperatures with different gas flow rates was studied. The various parameters influencing the cell voltage, discharge current *etc.* are discussed.

Key Words: Molten Carbonate Fuel Cells; Influence of Operating Parameters; Temperature

1 Introduction

The molten carbonate fuel cell (MCFC) is a highly efficient, environment friendly power generation system ideally suited for use as distributed generator. Because of its ability to use reformed natural gas or coal-derived gases, it is ideally suited for cogeneration of power. World wide, the MCFC technology is entering the 0.1 to 1.0 MW demonstration phase for performance verification and to gain the operating experience[1-3]. Improvement of the endurance of the MCFC stack components with a performance longevity >1,000 h and a life span > 10,000 h still remains an important issue for its successful commercialisation[4]. R&D efforts are to be focused in this direction to solve them. Major achievements are still necessary to provide a safe basis for reliable performance of MCFC[5]. This paper describes the results on the Molten Carbonate Fuel Cell Development conducted at CECRI.

1.1 Basic Components and Cell Design

A schematic diagram of a Molten Carbonate Fuel Cell (MCFC) and the components are shown in Fig. 1. The basic cell materials for MCFC are reasonably well defined and discussed[6,7]. Typically, both the porous anodes and cathodes are made from nickel powder. The carbonate electrolyte is supported in a matrix of lithium aluminate known as "Electrolyte tile"[8]. The operating temperature of MCFC is generally 923 K. A mixture of Li_2CO_3 and K_2CO_3 (62:38 mole %) is usually recommended as the electrolyte. The ohmic resistance is reported to be relatively low for the above composition[9]. The anode plaque is about 0.5 to 1 mm thick with 60 to 70 % porosity and a mean pore size of 5 μm[10]. The anode is made up of Ni dispersed with Cr, Al, and oxides of Al or Mg to prevent creep and to increase the resistance to sintering[11]. The cathode plaque is about 0.4 to 0.7 mm thick with 70 to 80 % porosity and a mean pore size of 10 μm[12]. The nickel cathode gets lithiated *in situ* inside the cell[13]. The electrodes and matrix materials are fabricated either by compaction, slurry casting or tape casting techniques followed by sintering[14]. Nickel or stainless steel (SS) current collectors support the electrodes.

2 Experimental – Component Fabrication

The overall goal of this task is to prepare the anode, cathode and electrolyte matrix structures, which will result in improved cell performance. Improvements in the tape

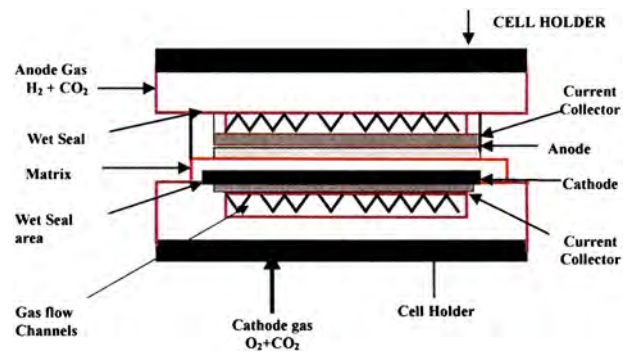

Fig. 1 Components of single Cell MCFC

E-mail: rpraman@rediffmail.com

casting process was attempted to optimize the factors governing the process. Among these studies, significant attempts were made towards development of dual porosity with two layers incorporating the bubble pressure barrier (BPB) layer to reduce the gas crossover between the anode and the cathode and to reduce the matrix cracking by adding fibre reinforcement. In addition, significant trials were also made to improve the cell design after testing them in a single cell assembly.

2.1 Anode Development

Our experiments have indicated that the electrodes formed from carbonyl Ni powder type 123 consisting of spherical particles (with 4-7 μm) have an average pore dia of 3-6 μm, whereas, the electrodes formed from carbonyl Ni powder type 255 (av. particle size 3-4 μm) have a pore diameter above 5 μm but below 10 μm. The average porosity values of the nickel electrodes were in the range 40-60% formed from type 123 Ni powder compared to the electrodes formed from type 255 Ni powder (in the range 60-80%) depending upon the sintering temperature. For both the types of Ni powders, the overall porosity values were found to decrease by increasing the sintering temperature[15]. The addition of Cr (10 wt%) to both the 123 and 255 powders had very little effect on the resulting electrode characteristics. There was a shift in widening of the larger pore diameter region.

2.1.1 Tape Casting Process

INCO Ni 255 was selected for the preparation of anodes for MCFC. Nickel powder with particle size in the range 9 – 13 μm was used. Both aqueous and non-aqueous tape casting process was employed for the preparation of thin, flexible green sheets. The typical composition ratios employed in these process is reported in Table I. The details of the exact compositions of the slurry, milling and the tape casting processes are proprietary. The slurry was then de-aired for 15 min., cast over a glass plate using a doctor's blade assembly and allowed for drying at room temperature for durations exceeding 12 h.

Table I

Composition and Physical Characteristics of Green Nickel Tapes with Additives

Property	Aqueous Process		Non aqueous Process		Non aqueous with fibre reinforcement	
Substrate	Ni (δ)	Ni (δ)	Ni	Ni	Ni	Ni
Binder	PVA	PVA	PVB	PVB	PVB	PVB
Plasticizer 1	Glycerol	Glycerol	PEG	PEG	PEG	PEG
Plasticizer 2	—	—	BBP	BBP	BBP	BBP
Defoaming agent	Silicone defoamer	Silicone defoamer	GTO	GTO	GTO	GTO
Additive	alcohol	alcohol	CH	CH	CH	CH
Solvent	Water	Water	Toluene/Xylene	Toluene/Xylene	Toluene/Xylene	Toluene/ Xylene
Blade gap (mm)	2.59	2.59	0.743	0.773	0.951	0.86
Thickness (mm)	0.80	0.99	1.448	1.448	1.68	1.68
Shrinkage factor (%)	69.11	61.78	48.68	46.61	40.88	43.39
Green density (g/cc)	1.91	2.38	2.217	2.097	2.239	2.312
Binder/solvent	0.158	0.158	0.289	0.231	0.334	0.334
B/B+P	0.335	0.335	0.526	0.597	0.301	0.301
Plasticizer/Solvent	0.314	0.314	0.260	0.156	0.526	0.526
Solid/B+P	—	—	2.631	2.985	2.631	2.631
B+P/Powder	—	—	0.38	0.335	0.38	0.38
B/P	0.504	0.504	1.111	1.481	1.111	1.111
Inorg/Inorg+Org	0.774	0.774	0.714	0.749	0.704	0.704
Packing factor	1.165	1.165	1.110	0.993	0.996	1.029
Tape quality	Leather like, smooth	Leather like, smooth	Smooth & flexible	Smooth & flexible	Good & flexible	Good & flexible

The slurry viscosity controls the physical properties of the tapes. Efforts were undertaken towards the development of tape casting process for larger area components. By this method the electrode tapes with thickness less than 0.5 mm were produced in the size range 30 x 40 cm^2. This requires not only slight modifications in the composition of the slurry, but also larger milling and tape casting time, thereby increasing the difficulty in obtaining tapes of uniform thickness.

The photograph (Fig. 2) shows the electrode tape of size 25 x 40 cm^2. The dried tapes were then characterized for shrinkage in thickness, during drying and green density values. These green tapes further characterized by TGA studies to determine the firing schedule during the sintering process[16]. The sintering schedule is indicated in Fig. 3.

Consequently the electrodes were sintered in hydrogen atmosphere at a slow heating rate of 1 K /min, with intermittent soaking stages at 423 K for 3 h and 673 K for 3 h to remove the inorganic constituents. The final sintering temperature was at 1073 K (1173 K for Ni-Cr) for 1 h and cooled to room temperature at 1 K /min.

2.1.2 Dual Porous Electrodes

The control of electrolyte retention is a key issue in determining the performance of porous electrodes[17]. There is an overlap between the pore size distribution in the electrodes and the pore size distribution in the electrolyte. It is generally an accepted hypothesis that smaller pores retain the electrolyte in preference to larger pores. For an electrode to perform well it must have some percentage of pores smaller than pores in the electrolyte matrix to retain the electrolyte. To develop such an electrode structure that would have good electrolyte retention properties, it was decided to form the dual porous electrode, with a fine layer (FPL) comprising mainly on average pore diameter of 4-6 μm facing the matrix, which will be less than the pore existing in the matrix (~7 μm) and another layer with an average pore in the range 7-10 μm. The coarse layer (CPL) will be facing the gas side and will be completely dry and free from electrolyte.

Hence dual porosity electrodes were successfully fabricated from the INCO Ni-123/255 combination by compaction sintering process. Fig. 4 indicates the pore size distribution curve of a dual porous electrode.

Typical pore size distribution of such an electrode had indicated that two distinct peaks were obtained one having pores of 3-5 μm and other with 5-12 μm. The total porosity of these plaques was generally about 65%. The overall porosity can also be increased by use of pore formers upto 10% in the coarse pore layer, while maintaining the overall pore size distribution without affecting the fine pore layer. The FPL acts as a barrier (BPB) between the anode and cathode gas. Table II indicates the physical characteristics of various anode materials prepared.

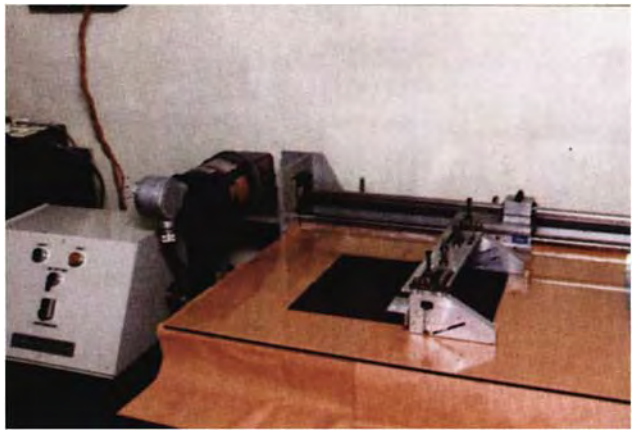

Fig. 2 Photograph of the nickel tape

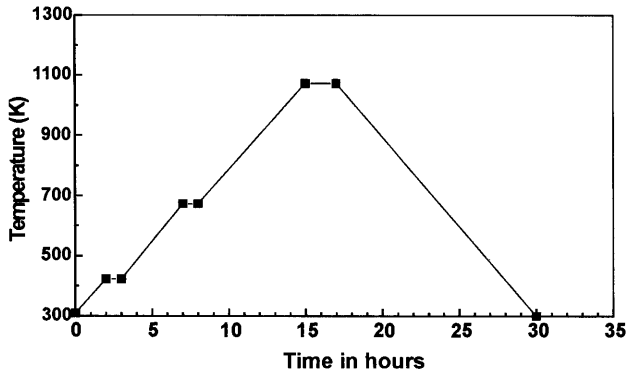

Fig. 3 Sintering schedule of green nickel tapes

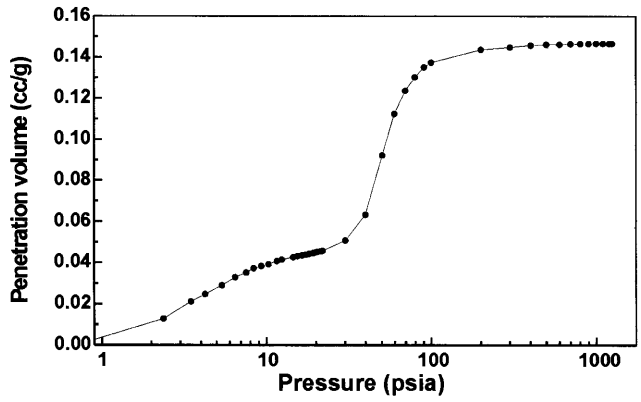

Fig. 4 Pore size distribution of a dual porosity electrode

Table II

Physical Characteristics of Anodes

	Ni-Al	Ni-Al	Ni-Cr	Ni-Cr	Dual layer	Ni-Al_2O_3	Ni-Al_2O_3	Dual layer	Ni-$LiAlO_2$	Ni-$LiAlO_2$
Blade gap (mm)	2.03	2.03	2.03	2.03	2.03	2.03	2.03	2.03	1.52	1.52
Green tape thickness (mm)	0.94	0.86	0.88	0.93	1.09	0.99	1.05	1.35	0.93	0.95
Shrinkage factor (%)	53.7	57.6	66.5	54.3	46.3	51.3	48.4	33.66	49.3	46.6
Sintered electrode thickness (mm)	0.85	0.73	0.63	0.81	0.86	0.92	0.84	0.96	0.71	0.75
Shrinkage factor (%)	9.57	15.1	17.3	12.5	21.5	6.77	17.6	28.34	26.4	21.1
Sintered electrode quality	good	good	good	good	good	good	good	good	good	good
Green tape density (g/cc)	2.44	2.27	2.88	2.76	1.57	2.27	2.33	1.52	1.72	2.00
Sintered Electrode density (g/cc)	2.05	2.08	2.96	3.09	2.06	2.30	2.46	2.01	2.16	2.41
Porosity (%)	63.4	66.2	56.0	55.5	74.6	62.6	62.7	68.5	57.7	55.6

2.2 Cathode Development

Cathode development efforts were directed towards fabrication and characterization of porous sintered NiO structures, reinforcement of porous Ni plaques and limited evaluations on alternate cathode materials. Nickel powder (INCO 255) was used to prepare the cathodes. Three different methods were adopted to prepare the lithiated nickel oxide cathodes for Molten Carbonate Fuel Cell (MCFC)[18]. In the first method, Ni electrodes with desired porosity were prepared and oxidized and lithiated inside the cell (*in-situ* method). Loose powder sintering, slurry casting and tape casting methods were followed to prepare the electrodes.

2.2.1 Preparation of Lithiated Nickel Oxide Catalysts

In the second method, the prelithiated nickel oxide powder was prepared by milling nickel powder and Li_2CO_3 in an organic medium (n-hexane). After drying at 373 K for 3 h, the solid state reaction was carried out by heating the sample at 923 K in air for 8 h. Five different compositions of lithiated nickel oxide samples were prepared by this method. This powder was ground well in an agate mortar and sieved through ASTM 325 mesh. Fig. 5 shows the schematic of the preparation of prelithiated nickel oxide catalysts and electrodes from it by the tape casting process (*ex-situ* method). The physical characteristics of the prepared lithiated nickel oxide samples are indicated in Table III. The *ex-situ* cathodes require higher sintering temperature above 1273 K. The tapes were reinforced using an SS wire mesh, which provided the mechanical strength during handling and also served as a current collector.

In the third method, the pre-lithiated nickel catalyst was formed into an electrode by tape casting technique

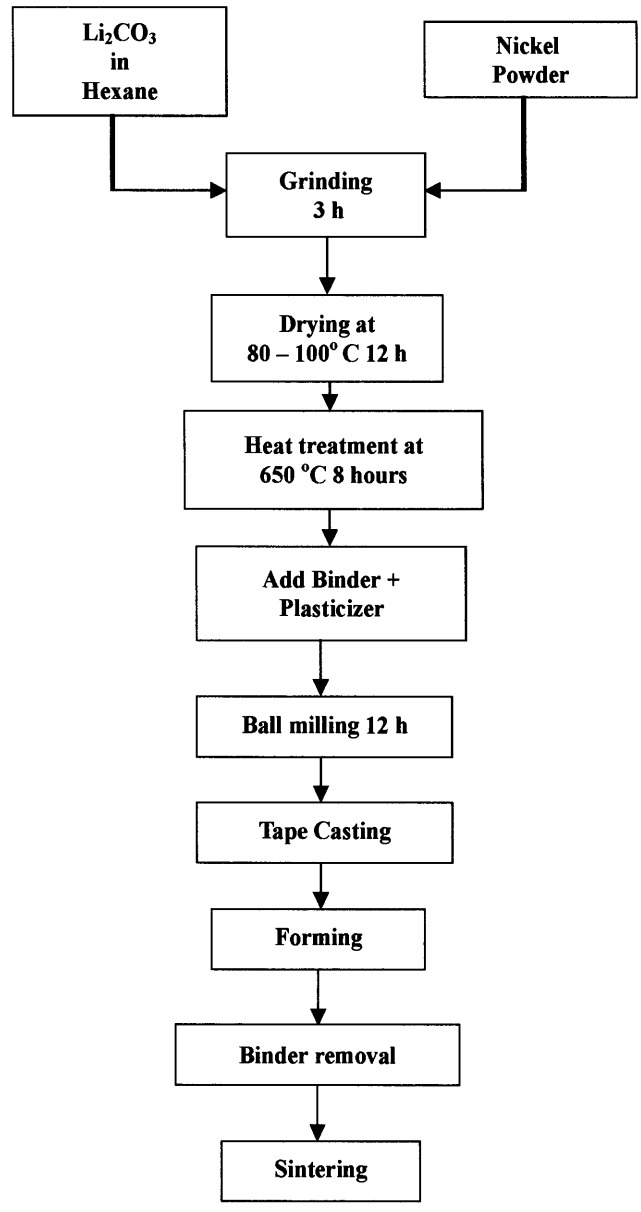

Fig. 5 Flow chart for the cathode fabrication process

and the electrodes were subjected to in cell or out of cell oxidation and sintering. The physico-chemical characterization of the catalysts and the electrodes were obtained by XRD and mercury porosimetry respectively. The green nickel tapes were characterized for the thickness, shrinkage factor, and density values. Table IV compares the characteristics of the various cathodes prepared by the above three methods. The performance of the electrodes was evaluated in single cells MCFC at 923 K.

The pore size distribution pattern for a typical electrode (Electrode No. 8 of Table IV) is indicated in Fig. 6. This Figure indicates that an electrode with a total porosity of 75%, the average pore size distribution is around 10 μm, which is more suitable as a cathode. The total penetration volume (pore volume), the average pore diameter, the total pore area and porosity values for the sintered electrodes have significance to the performance of cathodes. The electrodes with higher porosity have higher penetration volume and higher internal pore area (> 5 m^2/g). Further, it is noticed that INCO Ni-255 is good for the preparation of the cathodes with porosity in the range 75-80% with a mean pore size of 9-12 μm.

Table III

Characteristics of Lithiated Nickel Oxide Samples

Sl. No.	Li (atom %)	Ni	Surface area (m^2/g)	Av. Particle size (μm)	Lattice constant (A°)
1	1	99	5.12	3.50	4.1760
2	2	98	4.93	3.50	4.1712
3	5	95	4.91	3.90	4.1659
5	7.5	92.5	4.62	4.25	4.1614
6	10	90	4.30	4.75	4.1579
7	12	88	4.11	5.00	4.1535
8	15	85	3.81	5.50	4,1482
9	18	92	3.69	6.20	4.1428

Table IV

Characteristics of Nickel Electrodes Prepared by Loose Powder Sintering and Tape Casting Followed by Sintering Methods Used as in-situ Cathodes

Sl. No.	Green thickness (mm)	Sintered thickness (mm)	Shrinkage (%)	Green density (g/cc)	Sintered density (g/cc)	Porosity density (%)
Loose powder sintered Ni electrodes						
1		0.91	—	—-	1.66	64.11
2		0.78	—	—-	1.46	79.23
3		0.66	—	—-	2.87	62.34
4		0.76	—	—-	1.85	68.18
Tape cast and sintered Ni electrodes						
5	0.98	0.84	14.83	2.30	2.56	59.03
6	0.95	0.75	21.17	1.99	3.19	59.06
7	0.89	0.86	3.36	2.16	2.46	62.79
8	1.22	0.87	28.44	1.53	2.31	72.91
Pre lithiated, tape cast and out of cell sintered Ni electrodes						
9	1.12	0.90	19.20	1.52	2.22	71.91
10	0.97			2.64		
11	0.69	0.67		1.74	1.98	68.41
12	0.88	0.74	16.28	2.53	3.38	64.84
Pre lithiated, tape cast and in cell sintered Ni electrodes						
13	0.89			1.74		
14	0.81			2.78		
15	1.25			2.89		

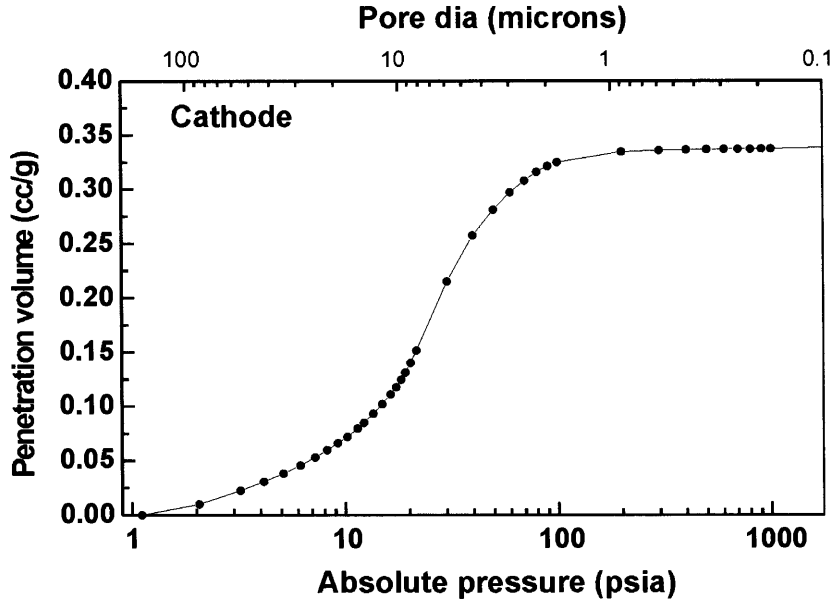

Fig. 6 Mercury penetration pore volume curve of the cathode

2.3 Electrolyte Matrix Development

The electrolyte matrix is the most critical component in MCFC. During cell operation, the tile becomes a paste like mixture of molten alkali carbonates and submicron $LiAlO_2$ support particles. The lithium aluminate powders prepared by the combustion synthesis using different fuels like urea, glycine were used. The method has resulted in a variety of $LiAlO_2$ samples with varying characteristics like density, surface area and particle size. The physical characteristics such as particle size and specific surface area of the different $LiAlO_2$ powders employed are given in Table V. For the preparation of molten carbonate fuel cell matrix, an admixture of different types of $LiAlO_2$ is prepared to avoid cracking and to retain stability during long term operation. This avoids the complications of segregation, agglomeration etc. The details are covered under a patented provisional specifications[19].

2.3.1 Tape Casting

Non-aqueous tape casting has been adopted for the matrix preparation to get smooth, flexible tape with uniform thickness. Milling was performed as a two step process in alumina jars using spherical alumina balls as grinding media with step-wise addition of ingredients for each stage. After the milling process, the slurry was filtered through a nylon mesh to remove the grinding media and any un-dissolved binder particles. Then, the slurry was de-aired for 15 minutes to remove the trapped air and cast over a glass plate using a doctor's blade assembly. The blade opening for all the castings was maintained at 1.50 mm. The cast body was dried below the room temperature for 12 h. After drying, the tapes were removed, cut into desired shapes and characterized. Tapes prepared by this milling process had smooth surface and are flexible (Fig. 7). Table VI shows the tape casting formulations using three different γ - $LiAlO_2$ powders, casting parameters and the physical characteristics of the green tapes.

2.3.2 Alumina Reinforced Matrix Preparation

Alumina fibres were incorporated into the $LiAlO_2$ matrix during the tape casting process to improve the mechanical strength and to minimize crack formation during cell testing. Table VII shows the composition, casting parameters and the physical characteristics of the matrix tapes prepared using two types of lithium aluminate powders with alumina fibre as additive.

2.3.3 Preparation of Electrolyte Impregnated Lithium Aluminate Matrix

Lithium aluminate powder prepared by the combustion synthesis and fine powders of Li_2CO_3 and K_2CO_3 were used for the study. Initially, $LiAlO_2$, Li_2CO_3 and K_2CO_3 powders were dry mixed for 6 h using alumina balls as grinding media. This mixture was then heat treated at 773-923 K in CO_2 stream for 2-4 h. After heat treatment, the mixture turned into a hard mass, which was then ground to get a free flowing powder. The powder was sieved through a 200 mesh and kept at around 373 K to

Table V

Physical Characteristics of γ-$LiAlO_2$ Powders

Powder type	Bulk density (g/cc)	Tap density (g/cc)	Av. particle size (μm)	Specific surface area (m^2/g)
γ-$LiAlO_2$ – 1	0.047	0.084	16.7	17.2
γ-$LiAlO_2$ – 2	0.019	0.059	15.2	10.5
γ-$LiAlO_2$ – 3	0.084	0.142	13.1	9.67
γ-$LiAlO_2$ – 4	0.030	0.053	16.1	17.5
γ-$LiAlO_2$ – 5	0.269	0.539	14.5	22.13
γ-$LiAlO_2$ – 6	0.285	0.527	17.8	15.7
γ-$LiAlO_2$ – 7	0.141	0.234	18.7	7.47

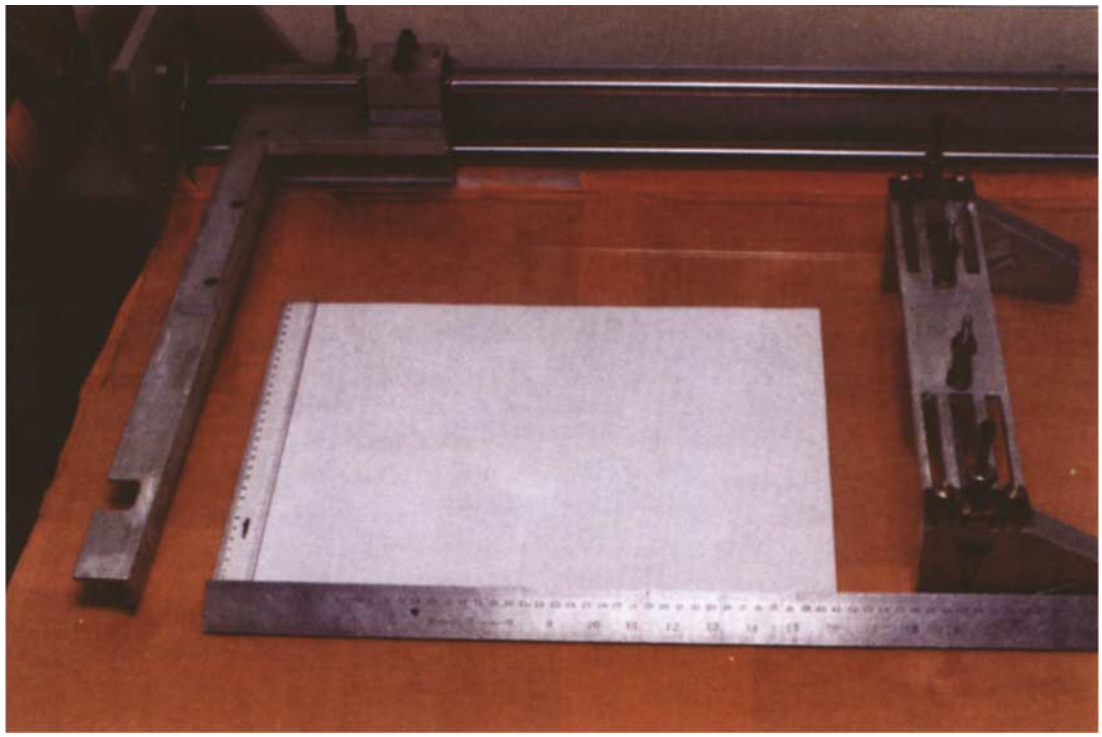

Fig. 7 Larger size matrix tape

Table VI

Compositions and Characteristics of Matrix Tapes made from Different $LiAlO_2$ Powders

	1	2	3	4	5	6	7
Blade Gap (mm)	1.448	1.448	0.93	1.448	0.682	0.736	0.750
Thickness (mm)	0.663	0.758	1.448	0.715	1.448	1.448	1.448
Shrinkage factor (%)	54.21	47.65	35.77	50.62	52.90	49.17	48.20
Green density (g/cc)	1.467	1.221	1.226	1.336	1.673	1.311	1.196
PVB/Solvent	0.252	0.252	0.158	0.303	0.132	0.289	0.346
Plasticizer/Solvent	0.217	0.190	0.226	0.195	0.188	0.216	0.260
B/B+P	0.538	0.570	0.412	0.608	0.412	0.571	0.571
Solid/B+P	1.537	1.631	1.303	1.738	1.303	1.142	1.142
B+P/Powder	0.65	0.613	0.767	0.575	0.767	0.875	0.875
B/P	1.165	1.330	0.702	1.553	0.702	1.554	1.332
Inorg./Inorg. + Org.	0.483	0.595	0.548	0.609	0.548	0.506	0.514
Packing factor	2.222	1.853	1.739	2.075	2.373	1.714	1.110
Tape quality	Good	Good, flexible	Good	Good	Good	Good, flexible	Good, flexible

Table VII

Compositions and Characteristics of Matrix Tapes using γ-$LiAlO_2$ Powder with Alumina Fibre

	1	2	3	4
Blade gap (mm)	1.448	1.448	1.448	1.448
Thickness (mm)	0.623	0.74	0.605	0.583
Shrinkage factor (%)	56.97	48.89	58.21	59.73
Green density (g/cc)	1.360	1.216	1.487	1.367
PVB/Solvent	0.242	0.202	0.385	0.385
Plasticizer/Solvent	0.156	0.130	0.20	0.20
B/B+P	0.608	0.608	0.639	0.639
Solid/B+P	1.738	1.738	0.959	0.959
B+P/Solid	0.575	0.575	1.042	1.042
B/P	1.553	1.553	1.776	1.776
Inorg./Inorg.+Org.	0.609	0.609	0.474	0.474
Packing factor	2.140	1.913	1.821	1.674
Tape quality	Flexible,	Smooth, good & flexible	Good, flexible flexible	Good, flexible

remove any moisture, which may affect the tape casting process.

Green, electrolyte impregnated, stabilized matrix structures were prepared by the tape casting technique[20]. Alumina fibre was first dispersed in methyl ethyl ketone (MEK)/ethanol (EtOH) solvent for 2 h using glycerol trioleate (GTO) as the dispersing agent. Then, lithium aluminate + eutectic mixture powder (40:60 wt%) (7-10 μm and 2.125 m^2/g) was added and dispersed for 2 h. This step was effective in removing any agglomerates initially present in the powder. After dispersion, the polyvinyl butyral (PVB) binder dissolved in minimum amount of the same solvent system was added and milled for another 4 h. Then, polyethylene glycol (PEG) and benzyl butyl phthalate (BBP) mixed plasticizers were added followed by 2 h milling. This slurry was subjected to de-airing and cast over a glass plate using a doctor's blade assembly with a blade opening of 1.5 mm and dried for 12 h. After drying, the tape was removed without any difficulty and cut in to desired size for further characterization. The tape was measured for average thickness at various points and the green density values were obtained by the Archimedes principle. The shrinkage values after casting and after heat treatment at different temperatures were also calculated.

2.3.4 Thermal Tests of the Green Matrix + Electrolyte Tapes

The eutectic electrolyte + $LiAlO_2$ matrix tapes were subjected to the following heat treatment steps in air and the density and shrinkage values at each step were calculated.

- room temperature (308 K) to 423 K at 3 K/min
- soaking time of 2 h.
- 473-573 K C at 3 K/min
- soaking time of 2 h
- 573-723 K at 3 K/min
- soaking time of 2 h
- 723-923 at 3 K/min

After measuring the density and shrinkage values at 923 K, the tape was kept at the same temperature for about 100 h to ensure no cracks has been formed at that temperature with a load of 1.5 kg/cm^2. Table VIII shows the volume, shrinkage and density changes of a typical matrix + electrolyte tape subjected to heat treatment at different temperatures.

Electrolyte tiles from terminated fuel cells and thermochemical tests were used to analyse the changes in the electrolyte amount and composition, surface area and morphology of the support. These will be useful to determine the cell endurance, to understand the failure mechanisms and to identify the probable modes of failure, including the cracking of the electrolyte matrix tiles. The cracking can be avoided by use of fibres for reinforcement of the matrix and the studies are helpful in optimizing the amount of reinforcing material. The observations are further supplemented by micrographic (SEM) analysis.

2.4 Laboratory Cell Tests

During the period a series of laboratory scale (3 cm^2 area) cell tests were undertaken to test the materials described in Tables II, IV and VI. Both the electrodes and matrix were cut into 3 cm^2 area circular shape and single cells were assembled and tested at different operating conditions[21, 22]. The experimental

Table VIII

Volume, Shrinkage and Density Changes of the Electrolyte+$LiAlO_2$ Matrix Tape Subjected to Heat Treatment

	308 K	423 K	573 K	723 K	923 K
Thickness (cm)	0.0657	0.065	0.063	0.062	0.060
Shrinkage factor (%)	——-	1.0654	4.109	5.631	8.675
Volume (cm^3)	0.225	0.222	0.216	0.212	0.205
Density (g/cc)	1.822	1.711	1.338	1.132	1.024

set up is shown in Fig. 8. The main purpose was to study the performance and stability with various electrolyte structures and electrodes, thereby to establish the parameters, which control the cell performance and stability. It is to ensure that single cell testing will provide meaningful comparison between various cells in order to ensure the improvements in the anode, electrolyte and matrix structures. Cells were tested with a single piece cathode current collector. The startup procedure on these cells was altered in an attempt affect the rate of *in-situ* Ni oxidation. The cells were discharged at various intervals of time at 873 and 923 K using the humidified fuel (H_2 + CO_2) and dry O_2 + CO_2. In all the cases, the OCV was 1.09 V, which is closer to the theoretical value.

Both the OCV and cell voltages at different temperatures, discharge c.d. for different gas flow rates were measured. Fig. 9 shows the anode gas flow rate on the cell performance at 873 K. Fig. 10 shows the anode gas flow rate on the cell performance at 923 K. Similarly the Fig. 11 shows the cathode gas flow rate on the cell performance at 873 K. Fig. 12 indicates cell data obtained when both anode and cathode gases are changed. The results from other experiments are also summarized in the Table IX. There is a significant dependence of OCV on the gas flow rate at 600° C. The observed OCV initially decreased and were almost the same at higher gas flow rates. At a constant value of cathodic gas flow rates, the change in the flow rates of anode gas resulted in a lower polarization initially, thereafter, and the polarisation was found to be higher. From the c.d. values it can be inferred that an optimum value of anode gas flow rate is 80+20 ml of H_2 + CO_2. The fuel utilization was maximum. In a similar manner from the polarisation curves obtained with the change of cathode gas at constant anode gas flow rate, the OCV steadily decreased, but the c.d. trend was in a similar fashion reaching a maximum at an optimum flow rate value. Any amount of increase of flow rate thereafter will not be helpful.

The influence of OCV in the temperature range 873-923 K was very small and did not follow any

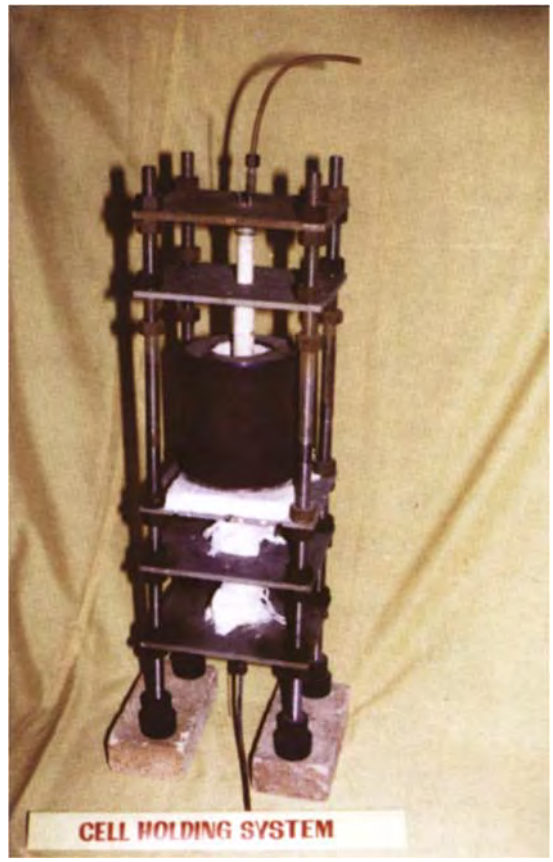

Fig. 8 Experimental set-up for single cell testing

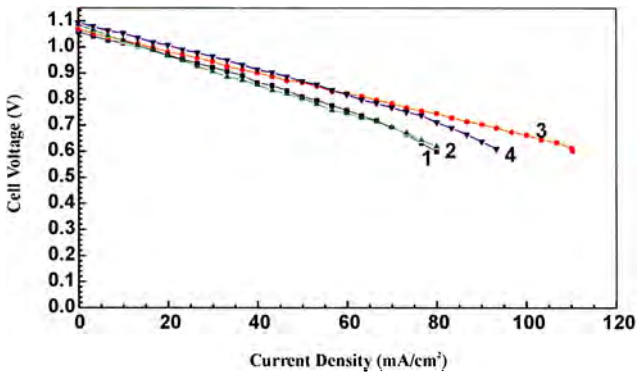

Fig. 9 Influence of anode gas flow rate on cell voltage at 873 K:
(1) H_2—40 + CO_2—10 ml/min;
(2) H_2—60 + CO_2—15 ml/min;
(3) H_2—80 + CO_2—20 ml/min and
(4) H_2—100 + CO_2—25 ml/min

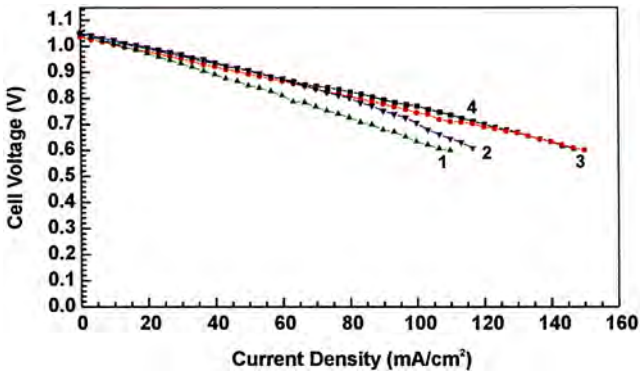

Fig. 10 Influence of anode gas flow rate on cell voltage at 923 K

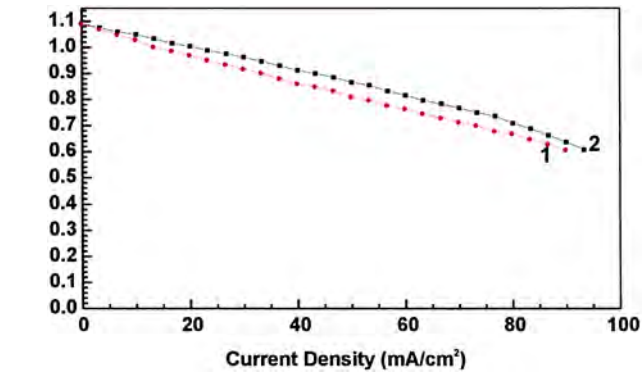

Fig. 11 Influence of cathode gas flow rate on cell voltage at 873 K

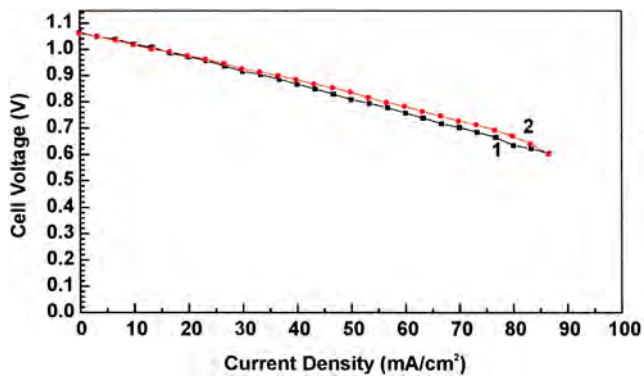

Fig. 12 Effect of anode and cathode gas flow rates on cell voltage at 873 K

order for different gas flow rates. Table X compares the OCV, CV, discharge c.d. values at the nominal and optimum gas flow rates at 923 K. At the normal flow rate, the OCV decreased with the temperature. But the discharge c.d. values were higher. At the optimum gas flow rate, the OCV was higher at 923 K. It is noticed from the polarisation curves that higher discharge c.d. can result in at 923 K than at 873 K.

The endurance test was carried out with optimum gas flow rates as shown in Figs. 13 & 14. The cell was tested for a period exceeding 500 h without any deterioration in its performance.

2.4.1 Post Test Analysis of Cell Components

Post test evaluation after 200 hour operation in 3 cm^2 size cells, revealed that the cathode was found to be slightly adhered to the electrolyte structure. Electrolyte structure was found to be apparently uniform. However there was no visible indication that poor contact existed in any particular area. The cathode was somewhat more rigidly attached to the current collector leading to considerable fracture during disassembly. Post-test data revealed that the cathode contained Li^+ in its volume. The results also indicated that the net electrolyte loss was about 12%. The gain in the anode and cathode was about 4 and 5% respectively. Hence cells were loaded to 120% of the theoretically calculated amount (i.e. ~105-120 mg/cm^2). The porosity of the cathode was lowered.

The performance of both metal reinforced NiO cathodes tape cast and in cell sintered was found to follow a similar trend. The *ex-situ* lithiated cathodes were more fragile than the *in-situ* oxidized cathodes. Hence the procedure was modified in such a manner that both the oxidation and sintering of prelithiated nickel tapes was done out side the cell in a programmed manner. This has resulted in a better

Table IX

Performance of Single Cell MCFC at Different Gas Flow Rates at 873 K

Anode gas flow rate (ml/min)	Cathode gas flow rate (ml/min)	OCV (V)	Cell voltage (V)	Current density (mA/cm^2)
40 + 10	33 + 66	1.017	0.607	80
60 + 15	33 + 66	1.036	0.601	100
80 + 20	33 + 66	1.054	0.604	110
100 + 25	33 + 66	1.056	0.609	120
80 + 20	25 + 50	1.063	0.603	90
80 + 20	40 +80	1.045	0.621	116
80 + 20	50 +100	1.040	0.609	146

Table X

Performance of Single Cell MCFC at Different Gas Flow Rates at 923 K

Anode gas flow rate (ml/min)	Cathode gas flow rate (ml/min)	OCV (V)	Cell voltage (V)	Current density (mA/cm²)
40 + 10	33 + 66	1.025	0.617	110
60 + 15	33 + 66	1.036	0.631	120
80 + 20	33 + 66	1.055	0.644	143
100 + 25	33 + 66	1.057	0.659	150
120 + 30	40 + 80	1.068	0.653	158
80 + 20	25 + 50	1.065	0.621	123
80 + 20	40 + 80	1.075	0.669	146
100 + 25	50 + 100	1.071	0.685	168
100 + 25	75 + 150	1.079	0.700	185

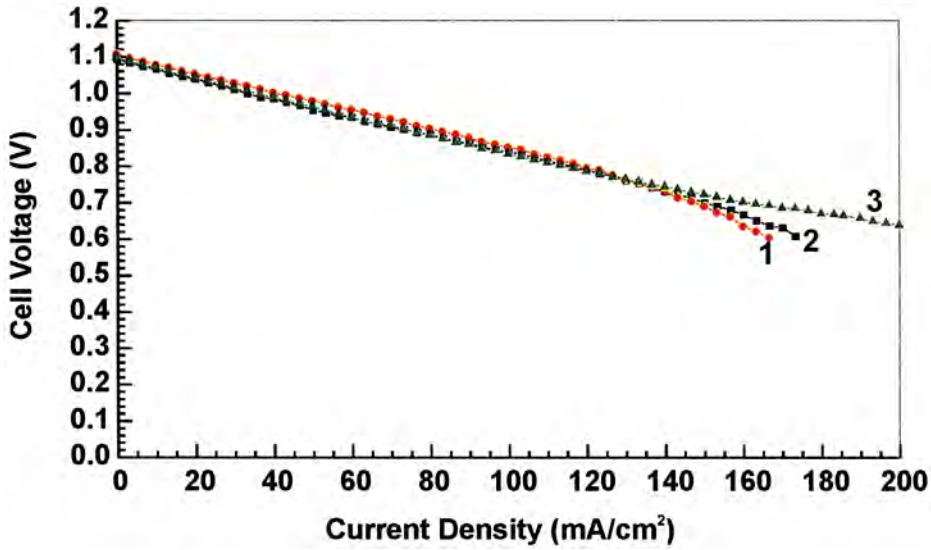

Fig. 13 Discharge comparison after 190, 200 & 215 hours of operation at 923 K at high gas flow rates (Table XI)

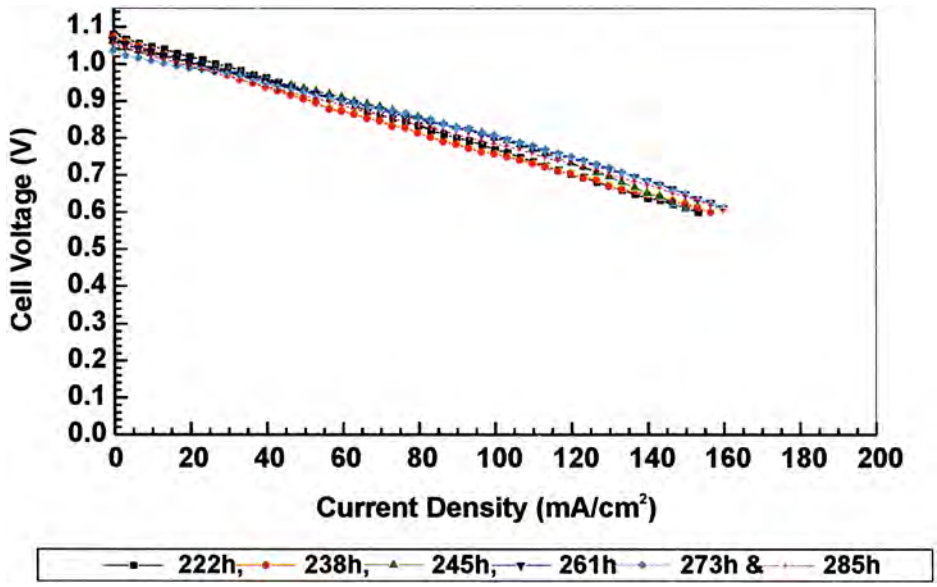

Fig. 14 Discharge with optimum gas flow rate after different times of operation at 923 K

control over the porosity and pore structure of the electrodes. These pre-sintered cathodes exhibited a performance value of 160 mA/cm^2 and the cells were also tested for duration exceeding 500 hours. The performance of the reinforced nickel cathodes are comparable to those obtained with standard non-reinforced cathodes.

Alumina fibre reinforced matrix exhibited better stability and thermal cycleability. Better stability of the matrix was also obtained with $LiAlO_2$ powders of different particle size and surface area.

2.4.2 Laboratory Cell Tests with Improved Components

Laboratory size cell tests at 923 K were also conducted by employing the dual porosity anodes, fibre reinforced matrix and *ex situ* lithiated, oxidized and sintered cathodes. The results are shown in Figs. 15 and 16. It was ensured that the test procedures were identical to the one reported earlier. The inlet composition was also changed to 34% H_2 + 24% CO_2 + 43% N_2 on the anode inlet and on the cathode inlet 15% O_2 + 55% N_2 + 30% CO_2. A gain in the performance of the cell by about 75-85 mV at 160 mA/cm^2 has been observed. Although this gain in performance is impressive, it is more important to understand the reasons.

From the single cell tests performed with various electrodes, matrix structures as indicated in the above Table XI, the following observations were made. Both anode and cathode gas composition and flow rates influence the cell voltage of MCFC. The cell current at any constant cell voltage was higher at high gas flow rates. Both OCV and CV were higher at O_2 rich cathodic gas composition. The loss in cell voltage was mainly dependent upon the anode gas flow rates. The

Table XI

Comparison of MCFC Cells at 923 K

Anode gas flow rate (ml/min)		Cathode gas flow rate (ml/min)			OCV	C.V at 150 mA/cm^2	c.d. at 0.7V
H_2	CO_2	O_2	CO_2	N_2	(V)	(V)	(mA/cm^2)
100	25	50	100	—	1.085	0.802	280
80	20	40	80	—	1.085	0.800	280
80	20	15	30	55	1.050	0.768	220
60	15	15	30	55	1.040	0.764	210
40	10	15	30	55	1.035	0.755	200
80	20	33	67	—	1.078	0.780	270
80	20	25	50	—	1.076	0.770	260
80	20	17	33	—	1.075	0.760	253
60	15	40	80	—	1.078	0.771	266
60	15	33	67	—	1.070	0.756	240
60	15	25	50	—	1.068	0.750	233
40	10	25	50	—	1.061	0.740	230
40	10	17	33	—	1.039	0.732	220

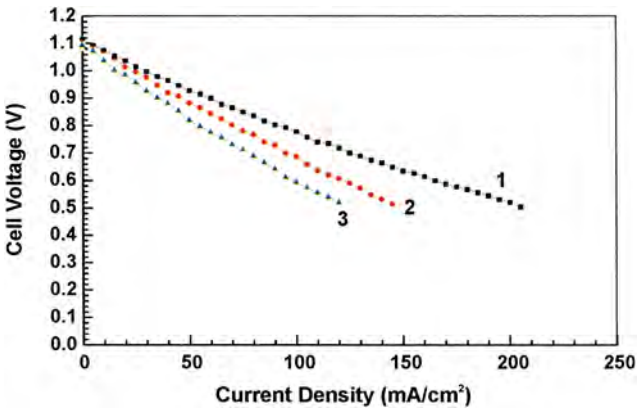

Fig. 15 Cell voltage of MCFC at different cathode gas flow rates at constant anode gas flow rate of H_2 + CO_2: 80+20 ml/min.

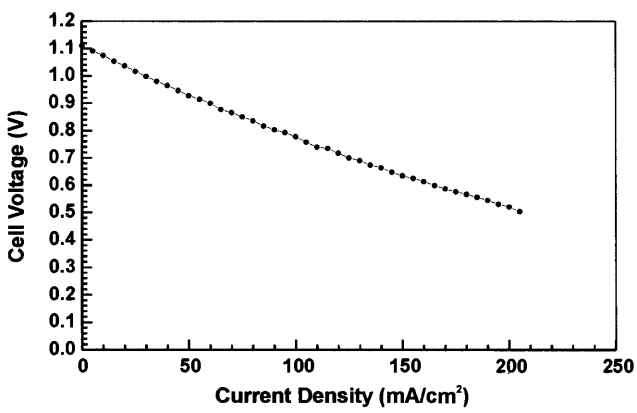

Fig. 16 Discharge Characteristics of MCFC at optimum gas flow rates

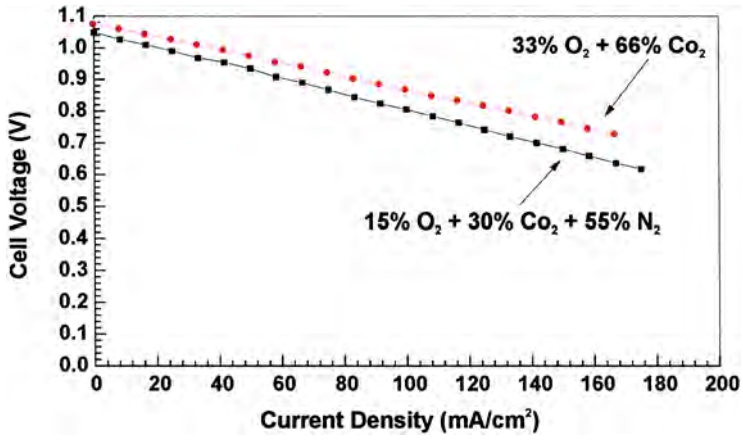

Fig. 17 Discharge comparisons of MCFC with different cathode gas compositions

overpotential loss on the cathode was almost 2 times that on the anode. The overpotential loss at the cathode was higher at N_2+ O_2+CO_2 gas, but independent of gas flow rates. C.d. values exceeding 250 mA/cm^2 is achievable with improved dual porosity electrodes and fibre incorporated matrices. During the course of 500 h test the cells were subjected to a thermal cycling tests also.

Conclusion

Significant progress has been made in the preparation of dual porous anodes, cathodes and electrolyte + matrix structures with improved quality, durability and better performance in MCFC cell conditions. Single cell tests with standard 3 cm^2 area revealed that high current densities ~250 mA/cm^2 are achievable. Dual porous anodes with fine pore layer acting as the bubble pressure barrier layer were found to be better. The crack in the matrix was reduced to the minimum by the use of Al_2O_3 fibre for reinforcement and by use of $LiAlO_2$ powders with two different particle size and surface area. Current densities of 100 mA/cm^2 were achieved in laboratory size (150 cm^2) cells at a cell voltage of 0.7 V at 923 K. The preliminary results on standard cells indicate that a multicell stack can be tested with the above characteristics of the components fabricated.

References

2 K Ota *New Material for Fuel Cells A* (Ed. O Savadogo) Ecole Polytechnique de Montreal Montreal Canada (1997) 86

3 T Ishikawa and H Yasue *J Power Sources* **86** (2000) 145

4 J P P Huijsmans, G J Makkus Kraaij, G Rietweld, E F Sitters and Th J Reijers *J Power Sources* **86** (2000) 117

5 R Pattabiraman Material issues in the development of Molten Carbonate Fuel Cells (MCFC) Fundamentals *Proc Two Day Conference on Fuel Cell Technology*, Applications and Opportunities Engineers India Ltd Gurgaon New Delhi (26 & 27 Nov 2001)

6 *Fuel Cell Hand Book* (5th Edition) EG&G Services Parsons Inc. Science Applications International Corporation Under Contract No. DE-AM26-99FT40575 US Dept. Energy Office of Fossil Energy National Energy Technology Laboratory Morgontown West Virginia (October 2000)

7 *Final Project Report Development of Molten Carbonate Fuel Cells* A Report by CECRI Karaikudi - submitted to MNES, New Delhi (Sep 1999)

8 H C Maru, L Paetsch and A Pigeaud *Proc 1st Symp on Molten Carbonate Fuel Cell Technology* PV 84-13 The Electrochemical Society Inc. Pennington NJ (1984) 20

9 J R Selman and H C Maru *Advances in Molten Salt Chemistry* **4** (1981) 154

10 C D Iacovangelo *J Electrochem Soc* **133** (1986) 280

11 Ih Oh, S P Yoon, T H Lim and S W Nam *Denki Kagaku* **64** (1990) 497

12 N Q Minh *J Power Sources* **24** (1988) 1

13 C E Baumgartner, R H Arendt, C D Iacovangelo and B R Karas *J Electrochem Soc* **131** (1984) 2217

14 A Pigeaud, H C Maru, L Paetsch, J Dayon and R Bernard *Proc Symp Porous Electrodes, Theory and Practice* (Eds. H C Maru, T Katan and M J Klein) The Electrochemical Society Inc Pennington NJ USA (1984) 234

15 C Solaiyan, P Gopalakrishnan, S Dheenadayalan, I Arulraj, S Muzhumathi and R Pattabiraman *Ind J Chem Technol* **6** (1999) 48

16 G Prabhu, C Solaiyan, S Dheenadayalan, I Arul Raj, S Muzhumathi, R Chandrasekaran and R Pattabiraman *Bull Electrochem* **15** (9-10) (1999) 389

17 Y Iwasw, H Okada, S Kuroe, S Mitsushima and M Takeuchi *Denki Kagaku* **62** (2) (1994) 152

18 G Prabhu, S Dheenadayalan, I Arulraj, R Chandrasekaran and R Pattabiraman *Ind J Chem Technol* (8 May 2001) 204

19 *Indian Patent* 3153/Del/98 dated 28/10/98

20 G Prabhu, R Chandrasekaran and R Pattabiraman *4th International Symp New Materials for Electrochemical Systems* (July 9-13, 2001) (submitted)

21 G Prabhu, C Solaiyan, R Chandrasekaran and R Pattabiraman *Trans SAEST* **35** (2000) 145

22 C Solaiyan, G Prabhu, S Dheenadayalan, I Arulraj, S Muzhumathi, R Chandrasekaran, R Pattabiraman and M Raghavan *Trans SAEST* 36 (3&4) (2001) 83